

A New Class of HIV-1 Tat Antagonist Acting through Tat–TAR Inhibition

François Hamy,* Vincent Brondani, Andreas Flörsheimer, Wilhelm Stark, Marcel J. J. Blommers, and Thomas Klimkait‡

Pharma Research, Novartis Pharma Inc., CH-4002 Basel, Switzerland

Received December 2, 1997

ABSTRACT: The main transcriptional regulator of the human immunodeficiency virus, the Tat protein, recognizes and binds to a small structured RNA element at the 5' end of every viral mRNA, termed TAR. On the basis of published structural data of the molecular interactions between TAR and Tat-related peptides, we defined requirements for potential low-molecular weight inhibitors of TAR recognition by the Tat protein. In accordance with the resulting concept, a series of compounds was synthesized. In vitro evaluation of their potential to directly interfere with Tat–TAR interaction was used to define a new chemical class of potent Tat antagonistic substances. The most active compound competed with Tat–TAR complexation with a competition dose CD_{50} of 22 nM in vitro and blocked HIV expression in a cellular Tat transactivation system with an IC_{50} of 1.2 μ M. The close relation between structural features of the interaction between TAR and a new type of inhibitory agent, “In-PRiNts” (for inhibitor of protein–ribonucleotide sequences), such as CGP 40336A and those of the Tat–TAR complex was confirmed by RNase A footprinting and by two-dimensional NMR. Structural implications for the complex between this class of compounds and TAR RNA will be presented.

So far, the only clinical successes in the field of target-directed AIDS treatment have been achieved with drugs against two key enzymes in the HIV life cycle: nucleoside analogues or non-nucleosidic inhibitors of the reverse transcriptase (e.g. AZT, ddI, ddC, etc.) (reviewed in ref 1) and inhibitors of the HIV protease (saquinavir, indinavir, ritonavir, etc.) (reviewed in ref 2). Nevertheless, HIV research had been hampered in the past by the observation of rapid development of viral resistance against drugs targeting either one of these viral enzymes, which poses a major threat for drug efficacy (3–6). This limitation has boosted attempts to explore additional targets. HIV proteins that centrally regulate viral gene expression could represent good candidates (7, 8). Indeed, it has been clearly demonstrated that HIV regulatory proteins possess an essential role in the viral life cycle (9, 10), and good insights into their mechanism of action have been gained in the past years (11, 12). Tat as the main activator of viral gene expression mediates a powerful induction of the production of all viral transcripts (13–15).

Although Tat has been described to interact with various cellular cofactors (16–18), only its well-studied interaction with the highly conserved TAR RNA element has so far been demonstrated to be a key element of the mechanism of action for Tat (19–21).

TAR is a 60-nucleotide long stem–loop RNA, characteristic for the 5' terminus of every HIV transcript (22); it creates a unique structure, with which Tat protein forms a

1:1 complex (19–22). Formation of this specific complex is an absolute prerequisite for Tat function. Without a crystal structure of the Tat–TAR complex, the largest contribution to the understanding of this peculiar protein–RNA recognition has come from biochemical and NMR analyses of the interaction of Tat-derived peptides with TAR (22–30). Those studies have meanwhile allowed definition of the Tat recognition site on TAR down to the level of atomic groups (23). The presence of three unpaired pyrimidines generates a widened major groove in the A-form stem of TAR RNA (24–29). A direct molecular interaction then takes place between an arginine-rich region of the Tat protein, the unpaired uridine at position 23 (U₂₃), and base pairs on both sides of the bulge (22, 23). It is stabilized by salt bridges between the cationic amino acids in Tat and phosphate residues from both strands of TAR (22–26). All these structural features of TAR taken together now allow conversion of the primary Tat-binding RNA sequence into a defined binding pocket (24). Numerous studies have shown through deletions or mutagenesis that an impairment of Tat binding is associated with a loss of viral gene expression (20, 22). Moreover, we recently reported the identification of a peptide-related compound, which, as an exogenous, synthetic inhibitor, was able to block HIV replication by targeting the protein–RNA interaction (31). Such a “receptor/ligand” like situation lends itself to creating a structurally realistic and biologically relevant target for molecularly directed drug discovery. In this study, we report the utilization of structural information for design and synthesis of concept-based low-molecular weight compounds, and their profiling in biochemical (direct TAR binding) and cellular (Tat inhibition) assay systems.

* Corresponding author: Novartis Pharma, Inc., Postfach, K-125.3.09, CH-4002 Basel, Switzerland. Telephone: (+41) 61 696 5093. Fax: (+41) 61 696 2083.

‡ Current address: Department of Molecular Diagnostics, Institute for Medical Microbiology, University of Basel Medical School, Petersplatz 10, CH-4003 Basel, Switzerland.

MATERIALS AND METHODS

Chemical Synthesis. All synthesized compounds were purified by flash chromatography or by recrystallization and characterized by MS and ^1H NMR, and the purity of compounds was checked by HPLC and TLC. 6-Chloro-2-methoxyacridine derivatives (CGP 40336A, CGP 73631A, CGP 73633A, CGP 73636A, CGP 73637A, CGP 74356A, CGP 64360A, CGP 74362A, CGP 74364A, CGP 79238A, and CGP 79242A) were synthesized by heating 6,9-dichloro-2-methoxyacridine together with the corresponding aminoalkyldi-*tert*-butyloxycarbonylspermidine, -norspermidine, or -homospermidine intermediates with (2-aminoethyl)-1,7-(di-*tert*-butoxycarbonyl)-1,4,7-triazaheptane, 5-(*p*-aminomethylbenzyl)-1,10-(di-*tert*-butoxycarbonyl)-1,5,10-triazadecane, or 8-(2-aminopropyl)-1,15-(di-*tert*-butoxycarbonyl)-1,8,15-triazapentadecane, at 110 °C in phenol for 1 h. After workup, the Boc-protecting groups were split off by using 3 M HCl in ethyl acetate. CGP 74361A was synthesized in an analogous manner starting from 1,10-(di-*tert*-butoxycarbonyl)-1,5,10-triazadecane and 4-(bromomethyl)benzocyanide. 8-(3-Aminopropyl)-1,15-(di-*tert*-butoxycarbonyl)-1,8,15-triazapentadecane, 4-(3-aminopropyl)-1,7-(di-*tert*-butoxycarbonyl)-1,4,7-triazaheptane, 5-(*p*-aminomethylbenzyl)-1,10-(di-*tert*-butoxycarbonyl)-1,5,10-triazadecane, and the aminoalkyldi-*tert*-butyloxycarbonylspermidine, -norspermidine, or -homospermidines were synthesized in a manner similar to the procedure of Cohen et al. (32). (2-Aminoethyl)-1,7-(di-*tert*-butyloxycarbonyl)-1,4,7-triazaheptane was synthesized by stirring 2 equiv of 2-[[(*tert*-butyloxycarbonyloxy)imino]-2-phenylacetone nitrile and tris(2-aminoethyl)amine in THF at 0–5 °C over the course of 2 h. Acridinecarboxylic acid derivatives (CGP 43681A, CGP 73638A, CGP 72164A, and CGP 72163A) were synthesized by condensing acridinecarboxylic acids with the corresponding aminoalkyldi-*tert*-butyloxycarbonylspermidine moieties, respectively, with (2-aminoethyl)-1,7-(di-*tert*-butyloxycarbonyl)-1,4,7-triazaheptane, by using hydroxybenzotriazole and dicyclohexylcarbodiimide. The Boc-protecting groups were split off by using 3 M HCl in ethyl acetate; in the case of CGP 43681A, oxalic acid was used (reflux in 50% aqueous methanol for 23 h). Acridine-4-carboxylic acid was synthesized according to the procedure of Atwell et al. (33). The naphthalinimide derivatives CGP 41081A and mitonafide (CGP 72194A) were synthesized according to the procedure of Braña et al. (34). The acridine derivative CGP 78833A was synthesized in a manner similar to the synthesis of the 6-chloro-2-methoxyacridine derivatives. 1-(Acridin-9-yl)-1,4-diazabutane (CGP 73641A) was synthesized by heating 1,2-diaminoethane and 9-chloroacridine at 100 °C for 18 h.

Gel Mobility Shift Assay. Recombinant Tat protein was prepared as described (22). TAR duplex was prepared by annealing two synthetic oligoribonucleotides, T-14 (5'-GCUGCUCUCUGGCU-3') and T-17 (5'-AGCCAGAUUUGAGCAGC-3') (Genset, Paris, France). The crude oligoribonucleotides were purified on 20% polyacrylamide gels containing 8 M urea. The 14-mer strand of the synthetic duplex TAR RNA was labeled with T4 polynucleotide kinase using [γ - ^{32}P]ATP. The labeled 14-mer was annealed in the presence of 1.5 equiv of the unlabeled 17-mer by heating to 90 °C for 3 min followed by slow cooling to 0 °C. Binding

reaction mixtures (25 μL) contained 500 fmol (≈ 10000 cpm) of the labeled duplex TAR RNA, 20 nM recombinant Tat protein, and varying concentrations of test compound in TK buffer [20 mM Tris-HCl (pH 8.0) and 50 mM KCl, with 10 mM DTT and 0.1% Triton X-100]. The binding reactions were analyzed by electrophoresis on 8% nondenaturing polyacrylamide gels as described (22, 23). Following electrophoresis, the gels were either dried and exposed on X-ray film at -70 °C for 16 h or analyzed on a Phosphor-imager (Molecular Dynamics).

Cellular Transactivation Assay. The HeLaT4-derived reporter cell line SX 22-1 (35) was cocultivated with Hut/4-3 lymphocytes at a ratio of 3:1. Hut/4-3 cells are derived from Hut 78 cells after stable transfection with the proviral HIV-1 clone pNL4-3 (36); they constitutively generate infectious virus particles. Cocultivation of the SX 22-1 reporter cells with the HIV-1 donor Hut/4-3 results in rapid cell fusion within hours. Thereby, Tat protein from the HIV-1 donor enters the reporter cells and induces the endogenous HIV LTR lacZ gene present in the SX22-1 cells. After overnight cocultivation, the cultures were rinsed with PBS and then exposed to glutaraldehyde/formaldehyde (0.2%/2%) in PBS for 5 min. After removal of the fixative, cells were stained for cell-associated β -galactosidase activity using X-gal as a substrate. For photometric quantification, the fixed cultures were subsequently incubated with *o*-nitrophenyl galactopyranoside (ONPG) as a β -galactosidase substrate, which was enzymatically converted into the chromophore *o*-nitrophenol (ONP).

Cell Culture. SX22-1 cells were cultured in DMEM with 4500 mg/mL glucose and 10% fetal bovine serum (FBS), supplemented with penicillin (500 IU/mL)/streptomycin (500 $\mu\text{g}/\text{mL}$); Hut/4-3 cells were maintained in RPMI and 10% FBS, supplemented with penicillin/streptomycin and 10 mM HEPES.

Cell media, media supplements, PBS buffer, HEPES, and sera were purchased from Life Technologies (Paisley, U.K.). All fine chemicals came from Merck (Darmstadt, Germany).

RNase A Footprinting. 60-mer TAR RNA was obtained by *in vitro* transcription as previously described (22). After recovery from gel purification, TAR RNA was labeled at the 3' end by ligation to cytidine 3',5'-[5'- ^{32}P]bisphosphate ([^{32}P]pCp) using T4 RNA ligase (22). Reaction mixtures contained 300 pmol of 60-mer TAR RNA, 65 μCi [^{32}P]pCp (220 TBq/mmol), 40 units of T4 RNA ligase, and 40 units of RNasin in a buffer containing 50 mM Tris-HCl (pH 7.4), 3 mM DTT, 5 mM MgCl_2 , 50 μM ATP, 25 $\mu\text{g}/\text{mL}$ bovine serum albumin, and 5% (v/v) dimethyl sulfoxide. After incubation at 4 °C overnight, the labeled RNA was purified by phenol/chloroform extraction and precipitated twice with ethanol. A lane was obtained after diethyl pyrocarbonate (DEPC) treatment following the method of Peattie (37).

Enzymatic footprinting reactions were carried out in a 20 μL volume containing 20 mM Tris-HCl (pH 8.0), 50 mM KCl, and 10 mM DTT. Typically, 3 pmol of 3'-end-labeled TAR RNA was incubated with 0.000 05 unit of RNase A for 2 min on ice in the presence, or absence, of Tat or varying concentrations of compound. Reactions were stopped by addition of 2 mL of proteinase K (2.5 $\mu\text{g}/\mu\text{L}$)/2.5% SDS. Subsequently, TAR RNA was purified by phenol/chloroform extraction and ethanol precipitation. Pellets were resuspended in 5 μL of formamide gel loading buffer, heated to

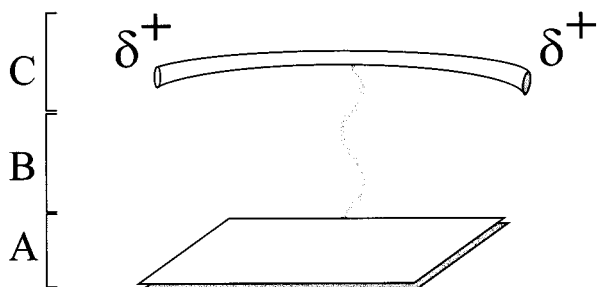


FIGURE 1: Schematic representation of the modular principle of the HIV inhibitors In-PRiNTs: (A) aromatic moiety for stacking, (B) aliphatic linker, and (C) polycationic anchor for contacts of the nucleic acid phosphate backbone.

90 °C, and rapidly chilled on ice prior to loading on a 10% acrylamide/8 M urea sequencing gel. Electrophoresis was carried out at 60 W, and gels were subsequently dried and exposed to X-ray film.

NMR Spectroscopy. 2'OMe-RNA oligonucleotides were synthesized and purified at Microsynth GmbH (Balgach, Switzerland). All NMR experiments were carried out on a Varian Unityplus 600 Spectrometer (600 MHz) equipped with a triple-resonance ^1H , ^{13}C , ^{15}N probe and z -gradients. Samples in 90% H_2O /10% D_2O were measured using the Watergate solvent suppression method. NOESY experiments (38) were carried out with mixing times of 50–300 ms. Clean-TOCSY experiments (39, 40) were carried out with a mixing time of 30 ms. Spectra were assigned on the basis of these homonuclear spectra (41) supplemented by a sensitivity-enhanced ^1H – ^{13}C HSQC spectrum (42) of TAR with natural abundance ^{13}C to allow discrimination between the H5–H6 cross-peaks originating from either uracil or cytidine bases. Data were processed with the VNMR 5.3 software distributed by Varian.

RESULTS

In Vitro Selection of Compounds. The concept for the identification of a Tat–TAR inhibitor was defined as outlined in Figure 1; the molecule should be tripartite and consist of a polyaromatic/heterocyclic moiety (part A) with the potential for a stacking interaction inside the cavity of TAR delimited by U23 as well as by bases below and above the bulge (A22 and G26, respectively), a feature providing partial positive charges for interaction with the phosphate backbone of RNA (part C), and a spacer to connect the stacking entity with the RNA binding part (B). We first focused on the deconvolution of the different possible combinations of the tripartite molecule by studying only the variation of the “stacker” moiety; whereas a polyamine moiety was fixed, which we chose to be spermidine for this oligocation has been described to possess nucleic acid binding properties by itself (43, 44), the linker length was arbitrarily set to a length of three carbons, and a series of different motifs were incorporated as the varying stacker candidates. Figure 2 shows a typical gel mobility shift competition assay using standardized conditions as previously described, to select inhibitors of the Tat–TAR interaction. Panel a depicts an autoradiograph of the controls in the absence of compound; the electrophoretic mobility of the ^{32}P -labeled TAR duplex (lane 0) is retarded by the addition of recombinant Tat protein (lane +Tat). Conditions were standardized to produce a pattern of equal band intensity at both gel positions in the

absence of inhibitor and were sustained throughout all competition experiments. Panels b–d show that, under these standard conditions, neither the oligocationic part alone (spermidine, panel b) nor any of the tested polyaromatic moieties (acridine, panel c; mitonafide, panel d) interfered with Tat–TAR complex formation. In sharp contrast, molecules utilizing the above elements, and connected according to our tripartite concept (e.g. mitonafide–spacer–spermidine, CGP 41081A, panel e; or acridine–spacer–spermidine, CGP 40336A, panel f), displayed potent competition. As can be directly deduced from the decreased band intensity of the complex, competition can be achieved already at low nanomolar compound concentrations. In contrast, the antimalarial drug quinacrine, which is structurally closely related to CGP 40336A (6-chloro-2-methoxyacridine–spacer–amine bearing side chain), was devoid of any activity, even at micromolar concentrations (panel g). In this first step of deconvolution, a series of polyaromatic entities (purines, naphthalinimide derivatives, etc.) were included as potential stacker elements for our tripartite concept (data not shown). Nevertheless, the potency of acridine derivatives to inhibit Tat–TAR interaction was in all tested cases superior to that of other heterocycles. Therefore, we selected the acridine ring system for the synthesis of a comprehensive series of compounds with variations of the length of both the linker and the oligocationic part. Those elements with depicted formulas are summarized in Table 1. Each compound of the series was assayed in a standardized gel shift experiment. To allow a direct side-by-side comparison of the activities of compounds, autoradiographs of the competition experiments were quantified by densitometry and expressed as CD_{50} values (compound concentration required to achieve a 50% decrease in intensity of the Tat–TAR complex band). The results are also reported in Table 1.

A comparison of these CD_{50} values makes it obvious that not every molecule, meeting the criteria of our concept, is necessarily a good inhibitor of the Tat–TAR interaction. Indeed, large activity differences were found throughout the series. On one hand, a small change in the structure can turn an active (inhibitory) compound into a completely inactive one (compare the CD_{50} values of CGP 40336A and CGP 74361A or CGP 74356A). On the other hand, markedly different compound structures can possess similar activities against Tat–TAR complex formation (compare CGP 74362A and CGP 73631A).

Although this set of data is not suitable for precisely inferring a structure–activity relationship and is not sufficient for the determination of a specific Tat–TAR inhibitor, several new features emerged from the table. (a) Variation of the linker length has only a mild effect on activity (compare compounds CGP 73637A, CGP 72164A, CGP 73636A, and CGP 79242A) except when its flexibility was highly constrained (CGP 74361A). (b) The polyamine moiety can be critical for Tat–TAR inhibition, e.g. when comparing CGP 73637A and CGP 74356A. (c) The position on the acridine ring system for a substitution of the linker seems to be important, e.g. comparing CGP 43681A (4-substituted) with CGP 40336A (9-substituted). (d) Independently of its length, the atomic composition of the linker is crucial for activity, as shown with the active compound CGP 40336A (linker type I, –NH–) in contrast to the

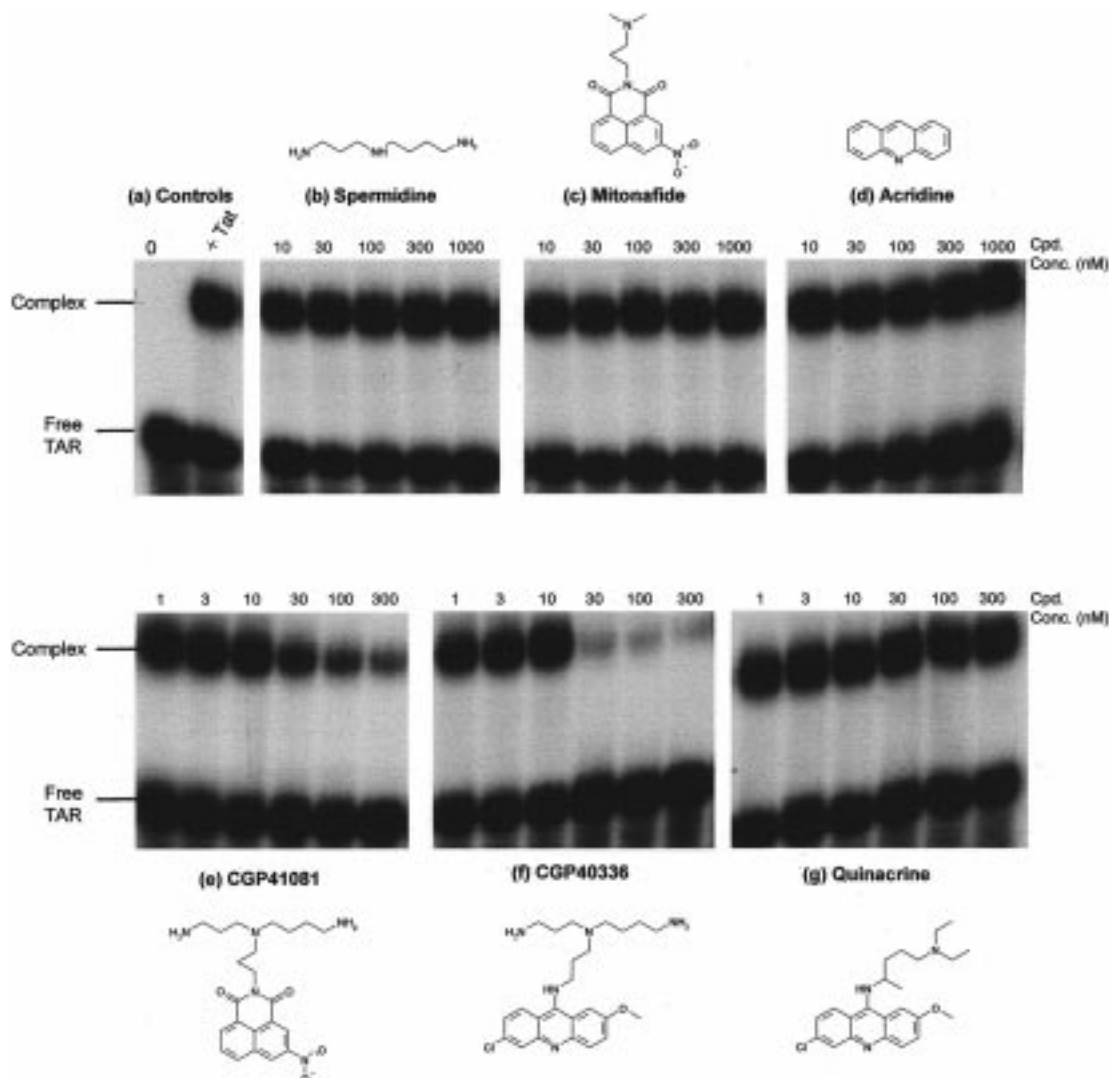


FIGURE 2: Biochemical selection of compounds by competition band shift assay. (a) Control gel mobility shift assays, showing gel migration of ^{32}P -labeled TAR RNA duplex (0) and its complex with 20 nM recombinant Tat protein (+Tat). Panels b–g show competition binding assays with the indicated compounds. Reaction mixtures contained 500 fmol of ^{32}P -labeled TAR RNA duplex, 20 nM recombinant Tat protein, and between 10 and 1000 nM compound, as indicated.

inactive CGP 72164A (linker type II, $-\text{CO}-\text{NH}-$). (e) Moreover, substituents on the ring system appear to influence the inhibition of Tat-TAR complex formation; e.g. compare CGP 78833A with CGP 40336A. These observations can provide a first basis for modeling of such specific drug-RNA interactions.

Tat Function Is Selectively Impaired in Cellular Settings. To verify whether the inhibition of Tat-TAR complex formation in vitro was predictive of inhibiting Tat-mediated transactivation in cells, we performed a cellular evaluation of the compounds in our fusion-induced gene stimulation (FIGS) assay (31, 35). In this system, Tat protein, constitutively expressed in the chronically HIV-1-infected donor cells, is rapidly transferred into an LTR reporter cell via HIV-mediated membrane fusion during cellular coculture. Within hours, Tat can induce β -galactosidase activity from an endogenous recombinant reporter gene. This reporter enzyme can then be used to localize the activated cells on the dish utilizing the strict cell association of the blue X-gal conversion product. Results of a typical experiment are shown in Figure 3. Panel a shows a picture of a culture of reporter cells alone. Upon coculture with the Hut/4-3 donor

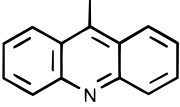
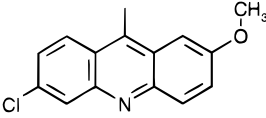
cells (panel b), the fusion between donor and indicator cells induces the formation of large syncytia which stains blue with the Tat-mediated expression of the LTR-driven β -galactosidase gene. When an inhibitor of Tat-TAR complex formation, e.g. CGP 40336A, was present in the medium of the coculture (panel c), we still observed formation of large syncytia, but in this case, after cell fusion, no Tat-dependent β -galactosidase expression and hence no blue stain were observed. This demonstrated that CGP 40336A was able to selectively block Tat-mediated transactivation without affecting the cell fusion event. Indeed, the FIGS system allows to readily discriminate between compounds interfering at the level of cell fusion (white, individual cells) or specifically at the level of Tat transactivation (white syncytia). Another advantage of the FIGS assay is that it lends itself to easy quantification in the extracellular buffer by a β -galactosidase-dependent conversion of diffusible ONPG to ONP and subsequent reading of the optical density at 420 nm. Using this readout, we can express β -galactosidase expression as a function of compound concentration. The graph depicted in panel d shows the results obtained with CGP 40336A. Using standardized conditions for the FIGS

Table 1: Synopsis of Associating Chemical Features with Compound-Related Activities in Biochemical and Cellular Assays^a

$$\begin{array}{c} \text{H}_2\text{N}-(\text{CH}_2)_x-\text{N}-(\text{CH}_2)_y-\text{NH}_2 \\ | \\ (\text{CH}_2)_z \\ | \\ \text{NH} \\ | \\ \text{R} \end{array} \quad \text{(I)}$$

$$\begin{array}{c} \text{H}_2\text{N}-(\text{CH}_2)_x-\text{N}-(\text{CH}_2)_y-\text{NH}_2 \\ | \\ (\text{CH}_2)_z \\ | \\ \text{NH} \\ | \\ \text{O}=\text{C} \\ | \\ \text{R} \end{array} \quad \text{(II)}$$

Connection of the polyamine part to the acridine moiety (**R**) via amino group (Type I) or via amide bond (Type II)

acridine type (R)	compound no.	linker <i>z</i> (type)	polyamine (<i>x</i> , <i>y</i>)	CD ₅₀ gel shift (nM)	IC ₅₀ FIGS (μM)	fusion inhibition (μM)	%Tox at 10 μM
	CGP 73641A	2 (I)	<i>b</i>	800	> 10	> 10	100
	CGP 73638A	2 (II)	2, 2	> 1000	> 10	> 10	—
	CGP 72164A	2 (II)	4, 3	> 1000	> 10	7	—
	CGP 78833A	3 (I)	4, 3	73	2	1	—
	CGP 72163A	3 (II)	4, 3	250	4	> 10	—
	CGP 74364A	2 (I)	2, 2	170	5	> 10	—
	CGP 73637A	2 (I)	4, 3	23	1	> 10	20
	CGP 74356A	2 (I)	4, 4	> 1000	6	8	90
	CGP 73631A	3 (I)	3, 3	31	2	> 10	50
	CGP 40336A	3 (I)	4, 3	22	1	> 10	30
	CGP 73633A	3 (I)	4, 4	44	3	> 10	50
	CGP 74359A	3 (I)	6, 6	82	2	> 10	100
	CGP 74360A	4 (I)	3, 3	83	1	> 10	—
	CGP 73636A	4 (I)	4, 3	76	3	> 10	50
	CGP 74362A	4 (I)	4, 4	27	1	> 10	—
	CGP 79242A	5 (I)	4, 3	39	1	2	—
	CGP 79238A	5 (I)	4, 4	30	2	10	—
	CGP 74361A	6 (I) ^c	4, 3	> 1000	3	> 10	100

^a Compounds belong to two main classes according to the acridinic moiety as indicated in column 1. Compounds are identified by the company's archiving system with CGP numbers. In column 3, *z* denotes the number of methylene units and the parentheses with I or II indicate the type of linker, as depicted above the table. In column 4, *x* and *y* refer to the number of methylene units from tertiary amine to the primary amino groups. CD₅₀ values are graphically determined values of those concentrations of compound required to mediate a 50% gel shift competition. IC₅₀ FIGS values reflect the compound concentration required for 50% inhibition of cellular, Tat-mediated LTR activation, determined by ONPG → ONP conversion. Fusion inhibition is judged by microscopic inspection and is reported as the lowest compound concentration at which a marked effect is observed. %Tox represents the compound with significant cytotoxicity at 10 μM, estimating the percentage of killed cells. ^b NH₂ group attached to the spacer. ^c Spacer = CH₂C₆H₄CH₂NH.

assay, all compounds were tested as described above, and for each of them, an IC₅₀ value was graphically determined and reported in Table 1. As was identified by microscopic inspection, several of the compounds had a direct impact on fusion. Table 1 summarizes the lowest compound concentrations at which this effect was observed. Cytotoxicity or cytostatic activity, which were also observed for several compounds, is shown in Table 1 by estimating the reduction in the percent cell number at a compound concentration of 10 μM.

Results of the FIGS assay demonstrated a good correlation between pure in vitro profiling of the compounds and their potency on a Tat-driven expression in a cell; i.e. as expected, compounds that were strong inhibitors of the in vitro Tat-TAR interaction (CD₅₀ band shift) were the ones showing a higher potency in inhibiting Tat-mediated transactivation of the reporter gene in cells. In agreement with the in vitro observation, the cellular system also reveals a sensitivity to modifications of the inhibitor candidates; small changes in the structure of a compound can have a dramatic effect on its activity. On the other hand, two markedly different compounds can be as active in Tat inhibition in a cellular setting.

However, at this point, we still could not draw any strict end point for a structure-activity relationship. Thus, in the

following studies, we decided to select CGP 40336A as the superior compromise between in vitro competition of Tat-TAR complex formation with a CD₅₀ of 22 nM and a Tat-selective, antagonistic activity in the FIGS system (IC₅₀ = 0.8 μM).

Tat and CGP 40336A Bind to the Same Region of TAR and Induce a Conformational Change. To verify that a direct binding to RNA is the method with which the compounds are inhibiting Tat-TAR interaction and to probe the modalities of such a binding, we performed RNase A footprinting experiments. TAR RNA was labeled at the 3' end and partially digested by RNase A either in the absence or in the presence of recombinant Tat protein or of the compound CGP 40336A. Figure 4 shows the autoradiograph of the corresponding sequencing gel. The patterns of digestion in the presence of either Tat or CGP 40336A (panel b) have to be compared with the control pattern of RNase A digestion (lane 0, panel a). We observed that binding of either Tat or CGP 40336A generated signal reductions at some positions and enhancements of cleavage at others. The affected bases were similar for both, as summarized on the RNA secondary structure, depicted in panel c; Tat protein protects TAR RNA from RNase A cleavage on essentially two regions facing each other in the TAR secondary structure: G26-A27 and C37-U40. The protection pattern upon binding of CGP

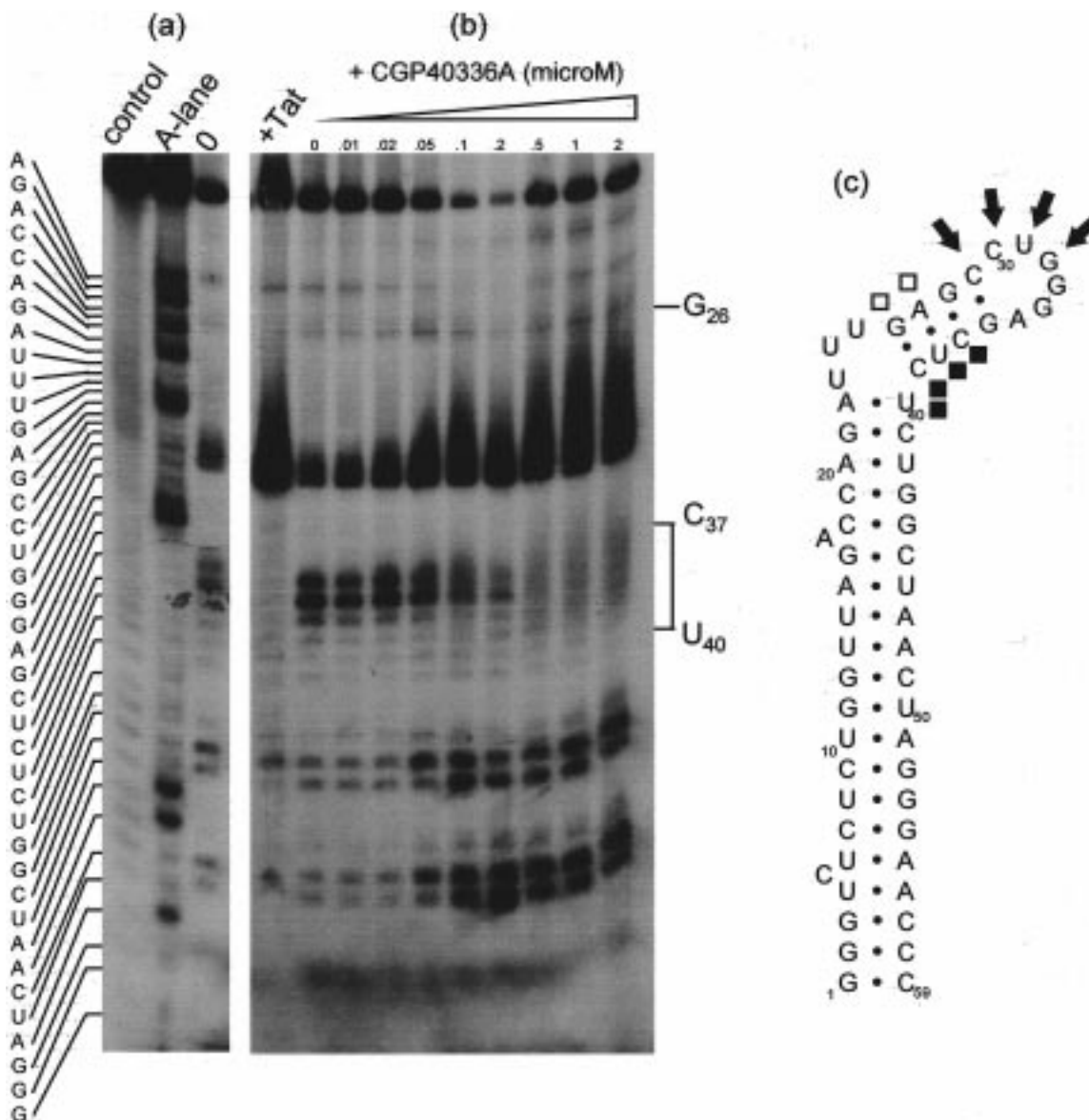


FIGURE 3: Site-specific binding of compound to in vitro transcribed, labeled TAR RNA. In panel a, the control lane denotes an untreated RNA sample. The A-lane shows a DEPC-treated sequencing ladder. In lane 0, a sample after treatment with RNase A is shown. In panel b, RNase A-treated samples were incubated either with 50 nM recombinant Tat protein (+Tat) or with increasing micromolar concentrations of CGP 40336A as indicated. (c) Secondary structure of the TAR transcript showing the sites of protection to RNase A upon the binding of Tat (\square) or of the compound CGP 40336A (\blacksquare). Black arrows indicate sites which display enhanced reactivity to RNase A upon ligand binding.

40336A shows protection only on one strand of TAR, i.e. at the C37–U40 site. More striking is the pattern for increased RNase sensitivity; the binding of either one, Tat or CGP 40336A, induced stronger cleavage in the region corresponding to the 5' end of the apical TAR loop (C29–G32). This provides good evidence that, in both cases, the binding to TAR induced a change of RNA conformation that renders these latter single-stranded regions even more exposed than in the unbound state and thereby accessible for the cleavage by RNase A. It is noteworthy that the pattern of cleavage enhancement (hence the change of conformation) is identical for Tat protein and the low-molecular weight compound CGP 40336A.

Two-Dimensional NMR. The results generated by our biochemical and cellular experiments prompted us to further study the interaction between compounds selected from Table 1 and TAR RNA, by employing NMR spectroscopy. For the NMR studies, the more stable 2'OMe-substituted ana-

logue of RNA was used, exploring the advantage of the additional methyl signals in the spectra (45), e.g. improved resonance assignment of the oligonucleotide spectra.

The 2'OMe RNA duplex analogue was tested for binding to recombinant Tat protein and had the same behavior (direct binding, competition) as the wild-type duplex TAR RNA (data not shown). The oligonucleotides could be shortened to the sequence displayed in Figure 5 without changes in the two-dimensional spectra, yet resulting in improved quality of the spectra.

All resonances in the H1'/H5–H6/H8 fingerprint of the bulged duplex have been assigned using standard sequential assignment procedures using NOESY and TOCSY experiments (41). In addition, the H1'–OMe region in the NOESY spectrum was explored, and a ^1H – ^{13}C HSQC was used to obtain an unambiguous discrimination between the H5–H6 cross-peaks, which correspond either to uridines or to cytidines. Assignments are indicated in Figure 5.

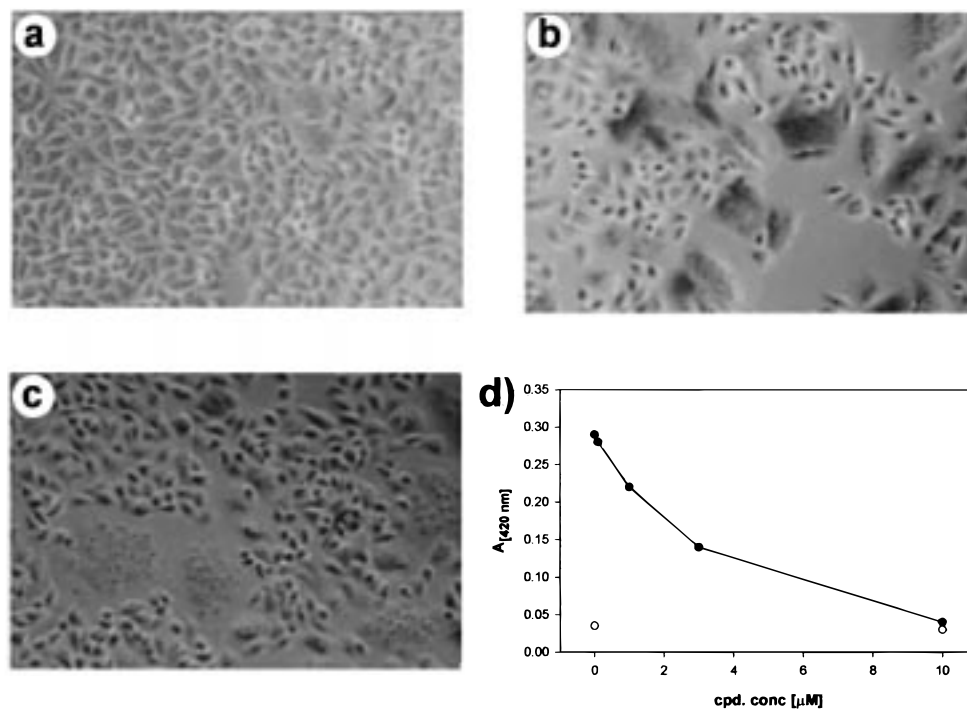


FIGURE 4: Evaluation of cellular activity in the FIGS assay: 24 h after coculture of chronically HIV-1-infected Hut4-3 cells with SX22-1 indicator cells (1000 \times). (a) Compound-treated control culture of SX22-1 cells. (b) Untreated coculture, showing extended syncytium formation with subsequent activation of the LTR-lacZ reporter by Tat. (c) Coculture treated with 10 μ M CGP 40336A. Note that cell fusion (generation of syncytia) is not affected, but Tat activity is completely suppressed. (d) Quantification of the ONPG reading in the β -Gal-driven ONPG conversion as a function of the concentration of CGP 40336A.

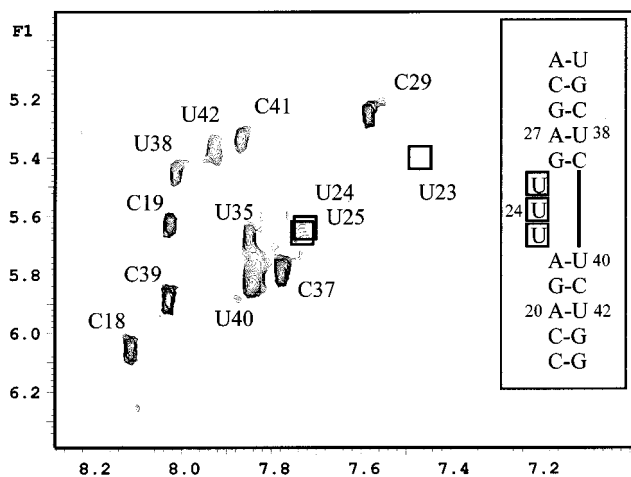


FIGURE 5: TOCSY spectrum of a 1:2 mixture of the acridine derivative CGP 79242A and the oligonucleotide duplex comprising the TAR bulge region. The resonance assignment of the H5-H6 cross-peaks is indicated. Boxes in the spectrum denote the position of cross-peaks of uncomplexed TAR, which are quenched upon addition of CGP 79242A. The oligonucleotide sequence is shown in the inset of the graph. Quenching of the signals at the bulge is indicative of a change in dynamics of this region toward the millisecond time scale upon inhibitor binding, suggesting site-specific interaction of CGP 79242A in the bulge region of TAR.

The conformational properties of the free 2'OMe duplex comprising the TAR bulge were similar to those previously published for TAR RNA (46, 47). For example, the base pairing as drawn in Figure 5 was confirmed by the presence of assigned imino proton signals which were shifted to the downfield region of the spectra. The imino proton resonance of U40 appears at 13.6 ppm, but is heavily broadened (24). In the following, the 2'OMe RNA bulged duplex will be referred to as "TAR".

Titration of the inhibitor CGP 79242A versus TAR resulted in a change of chemical shifts of the resonances of the ligand. In TAR, aside from the titrated signals, a significant number of signals broadened upon addition of the inhibitor and disappeared from the spectrum. Figure 5 displays the TOCSY spectrum of TAR after adding CGP 79242A to a ratio of 2:1 for RNA:compound. The cross-peaks corresponding to the base protons of the three bulged residues in uncomplexed TAR, the position of which has been indicated in the spectrum, vanished from the spectrum, whereas all other signals were still clearly visible. The quenching of these signals can be explained by conformational exchange on the millisecond time scale. This is likely to be caused by the interaction between inhibitor and nucleic acid, leaving its footprints in the spectrum.

Another example is given by the NOESY spectrum of the 1:1 mixture of CGP 40336A and TAR, displayed in Figure 6. NOE cross-peaks corresponding to the acridine derivative and cross-peaks corresponding to TAR were well separated. The signals corresponding to the small ligand CGP 40336A displayed strong negative NOEs, and the intensities were very similar to those recorded for TAR. At this relatively short mixing time (100 ms), only a few of the H1'-H6,8 connectivities (expected distance of about 3.5 Å) were detected. The NOEs detected for the acridine derivative in the complex are not detected in the absence of the nucleic acid as is expected on the basis of its molecular size (446 Da). Thus, in the presence of TAR, the inhibitor has a rotational correlation time which corresponds to that of the complex with TAR. Further detailed structural analysis is hampered by the quenching of NOEs, but it is interesting to note that some of the NOEs observed for the inhibitor in the complex were not present in the ROESY spectrum,

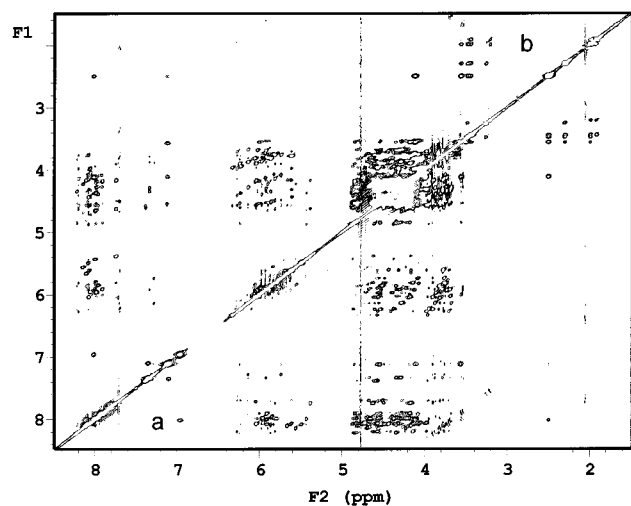


FIGURE 6: NOESY spectrum of the acridine derivative CGP 40336A in a 1:1 mixture with the 2'OMe-RNA bulged duplex (23-nucleotide), comprising the TAR bulge region. The mixing time was 100 ms. Strong NOE cross-peaks involving the resonances of the inhibitor in aromatic moiety (a) as well as the spermidine moiety (b) are indicators of binding.

recorded for the free ligand. On the basis of these NOEs, it is concluded that the TAR-bound compound has its OMe group in a peculiar spatial position. Moreover, a shift is observed for the 9-amino group of acridine, which could be demonstrated not to depend on pH (data not shown). Both observations could be important for tight complex formation and will be taken into account in discussing putative interaction models.

The titrations of both inhibitors to TAR followed by NOESY show quenching of cross-peaks similar to that shown by TOCSY (Figure 5). Interestingly, the broadening of signals is observed exclusively for the residues at or close to the bulge, particularly in the bulged strand. Strong effects were observed for residues A22-G28. Minor changes were found for residues C37-C41.

In conclusion, these NMR experiments provide direct evidence for a close association of the compounds with TAR. The changes of the fingerprint region upon titration show that the compounds bind specifically to the bulge region. This is the same region that is occupied by Tat-derived peptides (46, 47).

DISCUSSION

Several studies have now been reported on structure determination of complexes of TAR with Tat-derived peptides (24), peptoid (31), or argininamide (46). Although these reports are not fully congruent on several important points (like Arg fork or base triple), they are in good agreement on other aspects of the interaction: the specific binding of a ligand to TAR at its Tat-binding site induces a major conformational change that renders the major groove accessible for recognition. It is also now commonly agreed upon that a crucial early player in the Tat-TAR complex formation is the interaction of an arginine residue, which fits well into a binding pocket, formed by three critical residues of the bulge region: U23, A22, and G26 (24, 31). This initial binding step induces a structural rearrangement of TAR RNA that can then accommodate other functional groups of Tat protein for full and specific recognition. Our

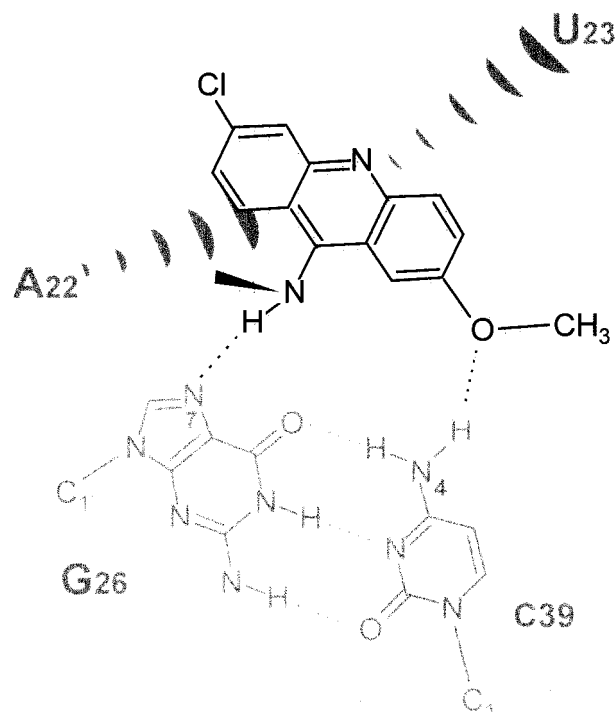


FIGURE 7: Schematic view of putative interactions between the acridine moiety and the binding pocket formed by TAR RNA. Aside from the compound stacking between A22 and U23 (as indicated), direct H bond contacts with both partners of the base pair G26-C39 could explain a specific orientation of the inhibitor molecule.

RNase A footprinting results, supported by NMR data, show that TAR RNA undergoes a similar structural change when bound to a representative of our class of compounds. Since the structure of the compounds contains neither arginine nor guanidinium groups, a different feature has to play this role, and our observations suggest that the heterocyclic moiety as a stacker could stabilize TAR RNA as does the arginine residue in the case of Tat. We refer to the most recent high-resolution structure described by Aboul-ela et al. (24) and to our recent observations on a peptoid-TAR interaction (31), which both find the insertion of the guanidinium group of arginine into the TAR binding pocket stabilized by stacking and cation- π^* interactions of the aliphatic side chain with surrounding bases. This unique positioning of the arginine side chain allows the ϵ NH of the guanidinium group to form a hydrogen bond with the N7 of G26. And this had been shown earlier to be critical for Tat-specific binding (22, 23).

In Figure 7 (to be considered only a sketch for better understanding of the drug-RNA interaction), we have attempted to summarize the details of potential interactions in agreement with our medicinal chemistry data.

For the described class of compounds, the simplest explanation supported by our data is that the stacking interaction can be mimicked (and probably improved) when an electron-deficient π -system such as the chloro, OMe-substituted acridine is replacing the aliphatic side chain of arginine in the binding pocket. Indeed, stable stacking interactions can occur between the polyaromatic ring of acridine and the cavity formed by bases U23, G26, and A22 (see the drawing in Figure 7). This would be in accordance with our observations of higher TAR affinity of compounds with an altered electron density in the acridine ring system,

mediated by the substituents Cl and OMe. Moreover, such a mode of interaction would place the NH group (position 9 of the acridine) perfectly at hydrogen-bonding distance of the N7 of G26 as shown in Figure 7. A similar, nonintercalating, base-pair parallel binding of 9-aminoacridine has been demonstrated in both X-ray and NMR studies of oligodeoxynucleotide complexes (48, 49). Such a placement of the acridine ring system could position the electron doublet of the OMe substituent as a donor for a H bond with the exocyclic amino group of C39 (Figure 7). Also, this could explain the observed weak binding of compounds that do not have a secondary amine at this position (linker II or quinacrine). As has been observed for argininamide ($K_d \sim 3 \mu\text{M}$) (28), our findings demonstrate that similarly an acridine ring system alone is not sufficient for strong binding. We therefore postulate that the TAR-inhibitor complex is further stabilized (and altered TAR conformation then "locked") by salt bridges between the positively charged polyamine function of the compound and phosphate groups of TAR RNA. In our previous report on a peptoidic TAR inhibitor (31), the specific binding of an N-Arg residue was further stabilized by a positive charge at the end of a long aliphatic side chain, able to reach across the major groove. Whereas NMR does not provide information about the phosphate backbone, the RNase A protection pattern supports a model in which the phosphate backbone of the pyrimidine-rich stretch facing the bulge is contacted. As summarized in Table 1, our determination of a structure-activity relationship could not identify a strict correlation between linker length or spacing of the charges on the polycation moiety and TAR inhibition. Therefore, we cannot make conclusions about the precise structural or sequential arrangement of the contacted phosphates. Thus, we hypothesize that there is not a unique pattern for phosphate recognition for the whole class, but compounds with different linker/polyamine geometry rather contact different pairs of phosphate groups. This flexibility of the target recognition increases the likelihood of unselective binding to other (structured) nucleic acids and could explain the cytotoxicity observed for some compounds at high concentrations. On the other hand, the identification of compounds with significantly lower toxicity under retention of full inhibitory activity strongly suggests that the uniqueness of the TAR structure (rather than sequence) can be specifically targeted. Although there is clearly room for improvement by chemical optimization, our In-PRiNTs compounds already at this stage are demonstrate to possess features of a specific molecular recognition through shape, ionic stabilization, and selective electrostatic interaction. Using a short peptoid, we have already established proof of the principle for Tat-TAR targeted HIV inhibition (31), and we believe that a further refinement of this new class of low-molecular weight agents, described in this study, can lead to the generation of novel and highly potent antivirals.

REFERENCES

1. Hammer, S. M. (1996) *AIDS* 10, S1-S11.
2. Vasudevachari, M. B., Battista, C., Lane, H. C., Psallidopoulos, M. C., Zhao, B., Cook, J., Palmer, J. R., Romero, D. L., Tarpley, W. G., and Salzman, N. P. (1992) *Virology* 190, 269-277.
3. Larder, B. A., and Kemp, S. D. (1989) *Science* 246, 1155-1158.
4. Balzarini, J., Karlsson, A., Perez-Perez, M. J., Camarasa, M. J., Tarpley, W. G., and DeClercq, E. (1993) *J. Virol.* 67, 5353-5359.
5. Schinazi, R. F., Larder, B. A., and Mellors, J. W. (1996) *Int. Antiviral News* 4, 95-110.
6. Condra, J. H., and Schleif, W. A. (1995) *Nature* 374, 569-571.
7. Graham, G. J., and Maio, J. J. (1990) *Proc. Natl. Acad. Sci. U.S.A.* 87, 5817-5821.
8. Sullenger, B. A., Gallardo, H. F., Ungers, G. E., and Gilboa, E. (1990) *Cell* 63, 601-608.
9. Kingsman, S. M., and Kingsman, A. J. (1996) *Eur. J. Biochem.* 240, 491-507.
10. Arya, S. K., Guo, C., Josephs, S. F., and Wong-staal, F. (1985) *Science* 229, 69-73.
11. Kao, S.-Y., Calman, A. F., Luciw, P. A., and Peterlin, B. M. (1987) *Nature* 330, 489-493.
12. Marciniak, R. A., and Sharp, P. A. (1991) *EMBO J.* 10, 4189-4196.
13. Sodroski, J., Rosen, C., Wong-Staal, F., Salahuddin, S. Z., Popovic, M., Arya, S., Gallo, R. C., and Haseltine, W. A. (1985) *Science* 227, 171-173.
14. Keen, N., Gait, M. J., and Karn, J. (1996) *Proc. Natl. Acad. Sci. U.S.A.* 93, 2505-2510.
15. Rittner, K., Churcher, M. J., Gait, M. J., and Karn, J. (1995) *J. Mol. Biol.* 248, 562-580.
16. Berkhout, B., and Jeang, K.-T. (1991) *Nucleic Acids Res.* 19, 6169-6176.
17. Wu, F., Garcia, J., Sigman, D., and Gaynor, R. (1991) *Genes Dev.* 5, 2128-2140.
18. Wu-Baer, F., Lane, W. S., and Gaynor, R. B. (1995) *EMBO J.* 14, 5595-6009.
19. Dingwall, C., Ernberg, I., Gait, M. J., Green, S. M., Heaphy, S., Karn, J., Lowe, A. D., Singh, M. S., Skinner, M. A., and Valerio, R. (1989) *Proc. Natl. Acad. Sci. U.S.A.* 86, 6925-6929.
20. Roy, S., Delling, U., Chen, C.-H., Rosen, C. A., and Sonnenberg, N. (1990) *Genes Dev.* 4, 1365-1373.
21. Sumner-Smith, M., Roy, S., Barnett, R., Reid, L. S., Kuperman, R., Delling, U., and Sonnenberg, N. (1991) *J. Virol.* 65, 5196-5202.
22. Churcher, M. J., Lamont, C., Hamy, F., Dingwall, C., Green, S. M., Lowe, A. D., Butler, P. J. G., Gait, M. J., and Karn, J. (1993) *J. Mol. Biol.* 230, 90-110.
23. Hamy, F., Asseline, U., Grasby, J., Iwai, S., Pritchard, C., Slim, G., Butler, P. J. G., Karn, J., and Gait, M. J. (1993) *J. Mol. Biol.* 230, 111-123.
24. Aboul-ela, F., Karn, J., and Varani, G. (1995) *J. Mol. Biol.* 253, 313-332.
25. Calnan, B. J., Tidor, B., Biancalana, S., Hudson, D., and Frankel, A. D. (1991) *Science* 252, 1167-1171.
26. Weeks, K. M., and Crothers, D. M. (1991) *Cell* 66, 577-588.
27. Cordingley, M. G., LaFemina, R. L., Callahan, P. L., Condra, J. H., Sardana, V. V., Graham, D. J., Nguyen, T. M., LeGrow, K., Gotlib, L., Schlabach, A. J., and Colonno, R. J. (1990) *Proc. Natl. Acad. Sci. U.S.A.* 87, 8985-8989.
28. Tao, J., and Frankel, A. D. (1992) *Proc. Natl. Acad. Sci. U.S.A.* 89, 2723-2726.
29. Tao, J., and Frankel, A. D. (1993) *Proc. Natl. Acad. Sci. U.S.A.* 90, 1571-1575.
30. Weeks, K. M., Ampe, C., Schultz, S. C., Steitz, T. A., and Crothers, D. M. (1990) *Science* 249, 1281-1285.
31. Hamy, F., Felder, E. R., Heizmann, G., Lazdins, J., Aboul-ela, F., Varani, G., Karn, J., and Klimkait, T. (1997) *Proc. Natl. Acad. Sci. U.S.A.* 94, 3548-3553.
32. Cohen, G. M., Cullis, P. M., Hartley, J. A., Mather, A., Symons, M. C. R., and Wheelhouse, R. T. (1992) *J. Chem. Soc., Chem. Commun.* 27, 298-300.
33. Atwell, G. J., Baguley, B. C., Denny, W. A., and Rewcastle, G. W. (1987) *J. Med. Chem.* 30, 664-669.
34. Braña, M. F., Castellano, J. M., Jiménez, A. J. M., Roldán, C. M., Santos, A., and Vázquez, D. (1980) *Cancer Chemother. Pharmacol.* 4, 61-66.

35. Klimkait, T., Stauffer, F., Lupo, E., and Sonderegger-Rubli, C. (1998) *Virology* (submitted for publication).
36. Adachi, A., Gendelman, H. E., Koenig, S., Folks, T., Willey, R., Rabson, A., and Martin, M. A. (1986) *J. Virol.* 59, 1157–1161.
37. Peattie, D. A. (1979) *Proc. Natl. Acad. Sci. U.S.A.* 76, 1760–1764.
38. Jeener, J., Meier, B. H., Bachmann, P., and Ernst, R. R. (1979) *J. Chem. Phys.* 71, 4546–4593.
39. Braunschweiler, L., and Ernst, R. R. (1983) *J. Magn. Reson.* 53, 521–558.
40. Griesinger, C., Otting, G., Wüthrich, K., and Ernst, R. R. (1988) *J. Am. Chem. Soc.* 110, 7870–7872.
41. Wijmenga, S. S., Mooren, M. M. W., and Hilbers, C. W. (1993) in *NMR of Macromolecules, A practical approach* (Roberts, G. C. K., Ed.) pp 217–288, IRL Press, Oxford.
42. Bodenhausen, G., and Reuben, D. J. (1980) *Chem. Phys. Lett.* 69, 185–189.
43. Feuerstein, B. G., Williams, L. D., Basu, H. S., and Marton, L. J. (1991) *J. Cell. Biochem.* 46, 37–47.
44. Schmid, N., and Behr, J.-P. (1991) *Biochemistry* 30, 4357–4361.
45. Blommers, M. J. J., Pieleas, U., and De Mesmaeker, A. (1994) *Nucleic Acids Res.* 22, 4187–4194.
46. Puglisi, J. D., Tan, R., Calnan, B. J., Frankel, A. D., and Williamson, J. R. (1992) *Science* 257, 76–80.
47. Aboul-ela, F., Karn, J., and Varani, G. (1996) *Nucleic Acids Res.* 24, 3974–3981.
48. Sakore, T. D., Reddy, B. S., and Sobell, H. M. (1979) *J. Mol. Biol.* 135, 763–785.
49. Woodson, S. A., and Crothers, D. M. (1988) *Biochemistry* 27, 8904–8914.

BI972947S